

NASA TECHNICAL NOTE



NASA TN D-5328

C.1

NASA TN D-5328



LOAN COPY: RETURN TO
AFWL (WIL-3)
KIRTLAND AFB, N MEX

REFRACTIVE INDEX - PARTICLE DENSITY
CORRELATION FOR NONEQUILIBRIUM
CESIUM PLASMAS PROBED BY A
MULTIFREQUENCY HELIUM-NEON LASER

by Richard B. Lancashire

Lewis Research Center

Cleveland, Ohio



REFRACTIVE INDEX - PARTICLE DENSITY CORRELATION FOR
NONEQUILIBRIUM CESIUM PLASMAS PROBED BY A
MULTIFREQUENCY HELIUM-NEON LASER

By Richard B. Lancashire

Lewis Research Center
Cleveland, Ohio

NATIONAL AERONAUTICS AND SPACE ADMINISTRATION

For sale by the Clearinghouse for Federal Scientific and Technical Information
Springfield, Virginia 22151 - CFSTI price \$3.00

ABSTRACT

The refractive index of a nonequilibrium cesium plasma is computed for the free electrons and the neutral atoms ($6S_{1/2}$ to $7P_{3/2}$ levels) at laser wavelengths of 0.6328, 1.1523, and 3.3914 μm . Densities of the neutrals were computed using quasi-steady-state solutions to the various level rate equations for typical thermionic diode conditions (initial cesium atom densities from 10^{15} to 10^{17} cm^{-3} and electron temperatures from 1500 to 3000 K). The dominant contributors to the refractive index are the ground-state neutrals and the free electrons. The results indicate the usefulness of the technique to measure local cesium atom densities accurately.

REFRACTIVE INDEX - PARTICLE DENSITY CORRELATION FOR
NONEQUILIBRIUM CESIUM PLASMAS PROBED BY A
MULTIFREQUENCY HELIUM-NEON LASER

by Richard B. Lancashire
Lewis Research Center

SUMMARY

An analysis of the refractive index of a nonequilibrium cesium plasma such as exists in a thermionic diode is presented. The index is computed for typical diode conditions for which the initial cesium density is in the range of 10^{15} to 10^{17} atoms per cubic centimeter and for electron temperatures between 1500 and 3000 K. These ranges allow for electron densities between 10^{12} and 10^{15} electrons per cubic centimeter. The refractive index is computed for individual species including the free electrons and the neutrals in the ground state and in excited states up to the $7P_{3/2}$ level. Population densities of the neutrals were determined using quasi-steady-state solutions to the various level rate equations. The wavelengths at which the index is calculated are those associated with the helium (He) - neon (Ne) laser that can be used as a plasma interferometric probe. The results are presented in an experimentally usable form and indicate that the laser interferometric technique is suitable to measure ground-state neutral atoms and free electron densities typically found in diodes. Excited neutral atoms appear to have a negligible effect on the observed refractive index under most conditions.

INTRODUCTION

The current need for information concerning the composition of the plasma contained within the interelectrode space of a cesiated thermionic diode has demanded that new plasma diagnostic techniques be investigated. Emission spectroscopic techniques have been used quite successfully heretofore (ref. 1). However, the application of these techniques is limited to plasmas where the condition of local thermodynamic equilibrium (LTE) exists. In the LTE model, it is assumed that the distribution of the population

densities of the various plasma particles is determined, at any point in time and space, by the local value of temperature that describes the distribution function of the species dominating the reaction ratio (i. e., the electrons). Only under situations of relatively high electron density is this condition realized in a cesium diode. That is, unless the electron density is of the order of 5×10^{14} per cubic centimeter or greater, departures from equilibrium can be significant.

The advent of the gas laser interferometer (ref. 2) has created new possibilities of probing the interelectrode space of a diode. It offers as good spatial resolution (ref. 3) as emission spectroscopy and is capable of measuring electron densities down to 10^{11} per cubic centimeter or lower (ref. 4) without relying on the existence of local thermodynamic equilibrium. The parameter that it measures is the refractive index of the plasma. Not only free electrons but also ground-state and excited-state neutrals can contribute to the index. The application of the technique, however, has been generally limited to inert gas plasmas, where the free electrons are the chief contributors to the index at the laser wavelengths used. Unless the neutrals far outnumber the electrons in this type of plasma, the contributions of the neutrals is negligible because of the large energy gap which exists between the ground state and the first excited state in the inert gases.

However, in an alkali vapor plasma, such as a cesium arc, a different situation exists. Not only ground-state transitions but also allowed first and higher excited-state transitions correspond to the wavelength range in which most gas lasers operate (0.5 to $3.4 \mu\text{m}$). Hence, these states must be considered when probing a cesium plasma with a gas laser interferometer.

The purpose of this report is to compute and determine the significance of the contributions to the refractive index of the species constituting a nonequilibrium cesium plasma. The data are computed for a nonequilibrium plasma since this is the state in which the thermionic converter operates. The wavelengths chosen for the computations are those of the widely used helium-neon laser, 0.6328, 1.1523, and $3.3914 \mu\text{m}$.

SYMBOLS

c	speed of light in vacuum, 2.9979×10^8 m/sec
E	energy measured from continuum, J
e	electronic charge, 1.602×10^{-19} C
f	oscillator strength
g	statistical weight
\hbar	Planck's constant, 1.0545×10^{-34} J-sec

k	Boltzmann's constant, 1.38054×10^{-23} J/K
m	electron rest mass, 9.1091×10^{-31} kg
N	particle density, cm^{-3}
n-1	refractive index
R	recombination coefficient, cm^6/sec
S	ionization coefficient, cm^3/sec
T	temperature, K
α	polarizability, m^3
ϵ_0	dielectric constant in vacuum, 8.85×10^{-12} $\text{C}^2/(\text{N})(\text{m}^2)$
λ	wavelength, μm
ω	radial frequency, sec^{-1}
ω_p^2	plasma frequency, $10^6 e^2 N_e / \epsilon_0 m$, sec^{-1}
Subscripts:	
e	electron
i, j, k	quantum state of atom
0	initial condition

METHOD OF CALCULATION

The determination of the refractive index of a plasma is made by summing all of the individual contributions of the plasma species (ref. 1). The index of a given species can be described in terms of a dispersion formula involving the characteristic absorption frequencies of the atom, or in terms of the polarizability, a frequency-dependent quantity defined as the dipole moment induced in the atom per unit applied electric field. The common expression for the refractive index is

$$n(\omega) - 1 = -\frac{1}{2} \frac{\omega_p^2}{\omega^2} - 5 \times 10^5 \sum_j N_j \alpha_j \quad (1)$$

where the first quantity on the right side is the contribution due to the free electrons. The second quantity is that due to all other species j . In a cesium arc discharge, the number of atoms in excited states can become appreciable, and negative terms corre-

sponding to induced emission to lower energy states have to be included in the dispersion formula. Hence,

$$n(\omega)-1 = -\frac{1}{2} \frac{\omega_p^2}{\omega^2} - 5 \times 10^5 \sum_j N_j \left(\sum_k \alpha_k + \sum_i \alpha_i \right) \quad (2)$$

where

$$\alpha_k = \frac{e^2}{\epsilon_0 m} \frac{f_{jk}}{\omega^2 - \omega_{jk}^2}$$

and

$$\alpha_i = \frac{e^2}{\epsilon_0 m} \frac{f_{ji}}{\omega^2 - \omega_{ji}^2} = - \frac{e^2}{\epsilon_0 m} \frac{g_i}{g_j} \frac{f_{ij}}{\omega^2 - \omega_{ji}^2}$$

The subscript k (on α) refers to upward transitions of j to k , and i refers to downward transitions of j to i . The foregoing definition of the polarizability α assumes that the difference between the probing frequency and a particular transition frequency is greater than the damping term (a line-broadening phenomenon) which would otherwise appear in the denominator (see ref. 3).

In order to determine the number of terms necessary for an adequate summation in equation (2), one must consider the relative magnitudes of the population densities N_j , the nearness of a given transition frequency to the probing frequency $\omega^2 - \omega_{jk}^2$, and the oscillator strengths of the various transitions f_{jk} . The fact that the frequency of a particular transition is very close to the probing frequency does not necessarily mean that that transition is the dominant factor in the contribution of that species to the refractive index. The reverse, of course, is also true. However, the upper excited states (i. e., those close to the series limit) in any gas are generally populated to a much lesser extent than those near the ground state, and thus their contribution to the total refractive index can be ignored.

The examination of cesium energy level tables (ref. 5), if only allowed transitions are taken into consideration, indicates that eight species besides the free electrons could possibly contribute significantly to the refractive indices at the designated probing frequencies. Those species are the ground state atoms and the excited atoms in the states up through the $7P_{3/2}$ level. Table I lists the wavelengths ($\omega = 2\pi c/\lambda$) and their respective oscillator strengths for both upward and downward allowed transitions from these

first eight energy states of cesium. Only the very highest energy states, with their corresponding minute oscillator strengths for lower level transitions, have been omitted from this table.

Table II is a compilation of the quantity, shown in equation (2) as

$$-\frac{1}{2} \left(\sum_k \alpha_k + \sum_i \alpha_i \right) = \frac{(n-1)_j}{N_j}$$

for the individual species at the three different laser wavelengths. The product of a tabulated value and its respective number density is the contribution of that species to the total refractive index. Note that many polarizability terms for the higher excited states have larger magnitudes than those for the ground-state terms. These tables indicate the sensitivity of the total refractive index to the species number densities. This fact is, of course, the primary reason for measuring the refractive index of a plasma.

The populations of the various energy levels are functions of the thermodynamic state of the plasma. If the plasma exists in a state of thermodynamic equilibrium (i. e., all species are characterized by the same temperature), the relation between the densities of the various states and the free electron density is given by the well-known Saha equation

$$N_{j\text{SAHA}} = \left(\frac{g_j}{2} \right) \left(N_e^2 \right) \left(\frac{2\pi\hbar^2}{mkT_e} \right)^{3/2} \exp\left(\frac{E_j}{kT_e} \right) \quad (3)$$

However, the plasma in a cesiated thermionic diode is not, in general, in thermodynamic equilibrium; although it can exist in a state of local thermodynamic equilibrium, if the electron density is sufficiently high ($>5 \times 10^{14} \text{ cm}^{-3}$). Maximum free electron densities of the order of 10^{15} per cubic centimeter are possible (ref. 1) in the plasma. However, densities several orders of magnitude lower are more representative and, therefore, substantial deviations from equilibrium are encountered. Hence, equation (3) fails to yield adequate values for nonequilibrium particle densities. For the purpose of computing the plasma refractive index, this report utilizes a method for determining nonequilibrium particle densities in which the rate of change of neutral concentration is equated to the net ion production rate:

TABLE II. - RATIO OF REFRACTIVE INDEX TO SPECIES
NUMBER DENSITY AT LASER WAVELENGTHS OF
0.6328, 1.1523, AND 3.3914 MICROMETERS

Species	Wavelength, λ , μm		
	0.6328	1.1523	3.3914
	Ratio of refractive index to species number density, $\frac{(n-1)_j}{N_j}$, cm^{-3}		
6S _{1/2}	-4.6331×10 ⁻²²	9.4344×10 ⁻²²	4.3730×10 ⁻²²
6P _{1/2}	-2.6249×10 ⁻²²	-5.9155×10 ⁻²²	49.8640×10 ⁻²²
6P _{3/2}	0.7739×10 ⁻²²	-3.8464×10 ⁻²²	-195.9200×10 ⁻²²
5D _{3/2}	32.3110×10 ⁻²²	7.4565×10 ⁻²²	-12.5300×10 ⁻²²
5D _{5/2}	-5.2077×10 ⁻²²	8.4110×10 ⁻²²	129.0000×10 ⁻²²
7S _{1/2}	-1.9284×10 ⁻²²	-2.2607×10 ⁻²²	306.3500×10 ⁻²²
7P _{1/2}	-0.9329×10 ⁻²²	-4.8360×10 ⁻²²	-208.6300×10 ⁻²²
7P _{3/2}	-1.2357×10 ⁻²²	-5.6971×10 ⁻²²	-132.2600×10 ⁻²²
Electrons	-1.7967×10 ⁻²²	-5.9575×10 ⁻²²	-51.6050×10 ⁻²²

$$\frac{dN_j}{dt} = \left(\begin{array}{l} \text{Net electron-neutral collision-} \\ \text{induced ionization and re-} \\ \text{combination rate} \end{array} \right) + \left(\begin{array}{l} \text{Net electron-neutral collision-} \\ \text{induced excitation rate for} \\ \text{atomic transitions} \end{array} \right) + \left(\begin{array}{l} \text{Net radiative decay rate} \\ \text{from atomic levels} \end{array} \right) + \left(\begin{array}{l} \text{Net radiative re-} \\ \text{combination rate} \end{array} \right) \quad (4)$$

When the total number of atoms in excited states is small, the set of equations (4) is considerably simplified. In that case, the rates into and out of each excited state are very large compared with the rate at which their population changes (refs. 6 and 7). There-

fore, the excited states assume quasi-steady-state populations while the ground state and electron (ion) densities change. Equation (4) produces an infinite set (i. e. , j level) of equations. However, reference 8 reduced the set to a finite number by stipulating the highest levels (those with binding energies < 0.14 eV) to be in local thermodynamic equilibrium, and thus their populations are given by equation (3). This approach allowed 26 nonequilibrium levels to be considered (each multiplet was coalesced into a single level). Following references 7 and 8, the time dependence of the system is then well described by

$$\frac{dN_j}{dt} = 0 \quad \text{for } 2 \leq j \leq 26 \quad (5)$$

$$-\frac{dN_e}{dt} = \frac{dN_1}{dt} = RN_e^3 - SN_e N_1 \quad \text{for } j = 1 \quad (6)$$

where R is the effective collisional radiative recombination coefficient, and S is the ionization coefficient. Ignored in these equations are atom-atom and atom-ion collisions because of their relatively low excitation and ionization rates compared with electron rates. Molecular processes are also neglected primarily because of recent experimental observations obtained from cesium diodes (refs. 9 and 10). The electron velocity distribution was assumed to be maxwellian, which appears to be a good approximation at temperatures greater than 2000 K (ref. 11).

The results of the computations in reference 8 yielded the contributions of the continuum and the ground state to the population of each level. These are the results that have been used in the present report to compute the populations of the lowest eight energy levels for electron densities of 10^{12} , 10^{13} , 10^{14} , and 10^{15} per cubic centimeter and for electron temperatures of 1500, 2000, 2500, and 3000 K. For the condition $N_e = 10^{15}$ per cubic centimeter, the plasma was assumed to have reached the equilibrium state. For the purposes of these computations, 100-percent trapping of the resonance transition radiation was assumed.

RESULTS AND DISCUSSION

The particle densities computed at the conditions stated previously were combined with their respective polarizability function from table II to obtain their contributions to the plasma index. In order to present these results in an experimentally feasible form, a quantity N_0 is defined as the initial total atom density. For a neutral plasma,

$$N_0 = \sum N_j + N_e \quad (7)$$

This density can be considered as that which is determined from the vapor pressure of the cesium and the gas temperature in the interelectrode space. This temperature is generally approximated to be a linear function of the emitter and collector temperatures. For normal cesium diode operation (e.g., see ref. 12), the values of N_0 will fall within a range between 10^{15} and 10^{17} per cubic centimeter. This range encompasses vapor pressures from 0.2 to 10.0 torr (26.7 to 1336 N/m²) and gas temperatures from 900 to 1800 K.

The computed refractive index values are plotted as a function of N_0 and electron temperature T_e and are presented in the following order: Figures 1 to 3 show the variation of the total or observed refractive index at three different wavelengths; figures 4 to 6 show the variation of the free electron refractive index; and figures 7 to 15 show the variation of the refractive index of the neutral particles including the ground state and the first two excited doublet states. Since the algebraic sign of the individual indices varies with species, only the absolute values are plotted. The actual sign may be obtained from the respective entries in table II.

In order to interpret the plots, certain conditions must be stipulated as to accuracy and range of experimentally observable quantities. At any of the three wavelengths, it has been shown (refs. 2 and 4) that the $\sum(n-1)$ can be experimentally observed to within $\pm 1 \times 10^{-8}$. This is a high degree of accuracy since, for typical plasma and interferometer dimension, the range of measurable values of $\sum(n-1)$ is between 10^{-8} and 10^{-5} . However, the value of N_0 is considerably less accurately known experimentally from vapor pressure measurements. In fact, a 5° to 10° error in vapor temperature measurement (cesium reservoir temperature) can cause a 20- to 40-percent error in the density value. It is therefore obvious from figures 1 to 3 that one of the quantities obtainable from a total refractive index measurement is a fairly accurate value of the initial cesium density. This conclusion is particularly valid when the electron temperature is below approximately 2250 K (figs. 1(b), 2(b), and 3(b)). At higher electron temperatures, either knowledge of the temperature (e.g., spectroscopic observation) or dual wavelength measurements would be necessary to determine N_0 .

Since the slopes of the curves in figures 1(a), 2(a), and 3(a) are not all one, other species besides neutrals have an influence on the total refractive index. The effect of the free electrons is small at 0.6328 μm , and it only becomes significant at 1.1523 μm when the electron temperature is above 2500 K. However, at a wavelength of 3.3914 μm , the free electrons become significant at temperatures greater than 2200 K. At around 2600 K, the electrons become the dominant contributor to the total refractive index at 3.3914 μm (fig. 3). Figures 4 to 6 show the individual contribution of the electrons. It is quite apparent that, in order to separate their effect from the total refractive index,

dual wavelength observations at $3.3914 \mu\text{m}$ and preferably at $1.1523 \mu\text{m}$ must be employed. On the basis of making an observation of $(n-1)_e$ of approximately 5×10^{-8} at $3.3914 \mu\text{m}$, the minimum electron density measurable would be about $9 \times 10^{12} \text{ cm}^{-3}$ per cubic centimeter. An added bit of information obtainable from figures 4 to 6 is the fractional ionization at various temperature and initial density conditions. The ratio of the ordinate to the abscissa at any point in these figures is proportional to the fractional ionization. The proportionality constant is obtained from table II. The maximum fractional ionization obtained in this manner is 26 percent. This definition of fractional ionization follows that of reference 11.

The effect of the ground-state neutrals is shown in figures 7 to 9. At the relatively low electron temperature of 2000 K, these curves are identical to the total refractive index curves. This indicates that the unexcited neutrals are the dominant species at these temperatures as far as interferometric measurements are concerned. At the higher temperatures and, in particular, at a wavelength of $3.3914 \mu\text{m}$, other species play an important part. Note also that, at higher initial cesium densities, the effect of other species diminishes. These conditions would correspond to cesium pressures of the order of 10 torr and/or low gas temperatures encountered near the collector surface in a diode.

In addition to the free electrons and the ground-state neutrals, excited neutrals could possibly have an effect on the total refractive index. Figures 10 to 15 present these effects for the three different wavelengths. Only the $6P$ and $5D$ states are plotted since they would have the highest densities of any of the excited states. As is evident from the figures, even these states offer little contribution to the total refractive index under most conditions. However, it does appear that care must be exercised when the $3.3914\text{-}\mu\text{m}$ wavelength is used for probing a plasma in which the electron temperature is approximately 2500 K or greater. In this temperature range and when the initial atom density is of the order of 10^{16} per cubic centimeter or greater, the contributions of the electrons and the $6P_{3/2}$ excited neutrals are about equal and are within an order of magnitude of the ground-state contribution. In this same range, the $5D_{5/2}$ excited neutrals have a contribution that is approximately one-fifth that of the $6P_{3/2}$ neutrals. It is, therefore, obvious that multiwavelength measurements are necessary if separation of the species effects is desired since the other wavelengths, 0.6328 and $1.1523 \mu\text{m}$, are sensitive only to the ground-state neutrals. At very high electron temperatures (3000 K) and at low initial atom densities (10^{15} cm^{-3}), the electrons can, though, contribute significantly at these wavelengths.

It is interesting to note the slopes of the curves in figures 10 to 12. They are essentially one for electron temperatures less than 2500 K. This is indicative of the fact that the populations of the first excited doublet states ($6P_{1/2}$ and $6P_{3/2}$) are proportional to the ground-state neutral density at a given temperature and thus follow the Saha relation of equation (3), or the well-known Boltzmann distribution. Since 100-percent trapping of

TABLE III. - POPULATION DENSITIES OF ENERGY STATES
 $7S_{1/2}$, $7P_{1/2}$, AND $7P_{3/2}$ AS COMPUTED AT VARIOUS
 ELECTRON TEMPERATURES AND DENSITIES

Electron temperature, T_e , K	Particle densities, cm^{-3}				
	N_e	N_0	$N_{7S_{1/2}}$	$N_{7P_{1/2}}$	$N_{7P_{3/2}}$
1500	10^{12}	1.844×10^{19}	1.096×10^{10}	1.032×10^8	2.065×10^8
	10^{13}	7.202×10^{19}	3.341×10^{11}	4.576×10^9	9.151×10^9
	10^{14}	1.295×10^{21}	1.877×10^{13}	3.428×10^{11}	6.856×10^{11}
	10^{15}	8.579×10^{22}	1.630×10^{15}	3.287×10^{13}	6.573×10^{13}
2000	10^{12}	4.682×10^{15}	3.275×10^8	6.659×10^6	1.332×10^7
	10^{13}	2.044×10^{16}	1.020×10^{10}	2.892×10^8	5.783×10^8
	10^{14}	4.264×10^{17}	5.596×10^{11}	2.255×10^{10}	4.510×10^{10}
	10^{15}	2.993×10^{19}	4.841×10^{13}	2.178×10^{12}	4.357×10^{12}
2500	10^{12}	3.060×10^{13}	3.769×10^7	1.191×10^6	2.381×10^6
	10^{13}	1.500×10^{14}	1.167×10^9	5.122×10^9	1.024×10^8
	10^{14}	3.323×10^{15}	6.279×10^{10}	4.087×10^9	8.173×10^9
	10^{15}	2.352×10^{17}	5.442×10^{12}	3.963×10^{11}	7.927×10^{11}
3000	10^{12}	1.957×10^{12}	8.613×10^6	3.621×10^5	7.240×10^5
	10^{13}	1.483×10^{13}	2.618×10^8	1.543×10^7	3.085×10^7
	10^{14}	2.188×10^{14}	1.389×10^{10}	1.245×10^9	2.490×10^9
	10^{15}	9.817×10^{15}	1.205×10^{12}	1.210×10^{11}	2.420×10^{11}

resonance radiation was assumed when the population densities were computed, this local equilibrium effect is to be expected. However, this equilibrium condition between the ground state and excited states does not extend to the second excited doublet states ($5D_{3/2}$ and $5D_{5/2}$) since the curves in figures 13 to 15 are nonlinear at all temperatures.

The contributions of the higher excited states considered in this analysis can be obtained from tables II and III. Table III lists the computed population densities of the $7S_{1/2}$, $7P_{1/2}$, and $7P_{3/2}$ states together with their respective values of N_0 . It is evident from these tables that, under almost all conditions, the contributions of these states to the total refractive index are negligible.

CONCLUSIONS

The analysis of a nonequilibrium cesium plasma indicates that the density sensitivity characteristics of gas laser interferometry can be effectively utilized. Although it is

highly sensitive to the unexcited neutrals in the plasma, the effect of the free electrons can be separated from the total effect through the use of multiple laser probing frequencies. Excited neutrals offer limited, if any, contributions to the refractive index that is observed and therefore can be neglected under most conditions.

One of the more important applications of the interferometric technique is the measurement of local values of cesium atom density which previously had to be inferred from reservoir vapor temperature measurements. A single experimental observation can obtain this measurement when the plasma electron temperature is of the order of 2200 K or lower.

It is apparent from the data presented that the electron temperature of the plasma, when it is above 2200 K, is a dominant factor controlling the experimental ability in separating the individual refractive indices of the species. If the electron temperature is known from some other source, such as emission spectroscopic measurements, the individual species effects are easily separable. However, temperature measurements obtained from the spectroscopic technique assume local thermal equilibrium conditions exist. Therefore, these measurements must not be regarded as being completely accurate. If all the laser wavelengths are used, nonequilibrium values of electron temperature may be obtained. The accuracy of these measurements would be controlled not only by the experimental limitations discussed previously but also by the validity of the analysis used to relate electron temperature, electron density, and neutral density (i. e., the Norcross and Stone analysis). Experimental verification is needed to determine this accuracy. Laser interferometry can yield particle densities directly and thus can shed some light on the validity of ionization and recombination analyses of thermionic diode plasmas.

Lewis Research Center,
National Aeronautics and Space Administration,
Cleveland, Ohio, May 6, 1969,
129-02-01-05-22.

REFERENCES

1. Griem, Hans R.: Plasma Spectroscopy. McGraw-Hill Book Co., Inc., 1964.
2. Ashby, D. E. T. F.; and Jephcott, D. F.: Measurement of Plasma Density Using a Gas Laser as an Infrared Interferometer. Appl. Phys. Letters, vol. 3, no. 1, July 1, 1963, pp. 13-16.
3. Lancashire, Richard B.: Study of Plasma Diagnostics Using Laser Interferometry with Emphasis on Its Application to Cesium Plasmas. NASA TM X-1652, 1968.

4. Fein, M. E.; Cherrington, B. E.; and Verdeyen, J. T.: A Laser Heterodyne System for Plasma Diagnostics. Scientific Rep. No. 1, Univ. of Illinois (NASA Grant NGR 14-005-037), 1967.
5. Moore, Charlotte E.: Atomic Energy Levels. Vol. 1. Circular 467, National Bureau of Standards, June 15, 1949, pp. 124-127.
6. Bates, D. R.; Kingston, A. E.; and McWhirter, R. W. P.: Recombination Between Electrons and Atomic Ions. I. Optically Thin Plasmas. Proc. Roy. Soc. (London), Ser. A, vol. 267, no. 1330, May 22, 1962, pp. 297-312.
7. Bates, D. R.; Kingston, A. E.; and McWhirter, R. W. P.: Recombination Between Electrons and Atomic Ions. II. Optically Thick Plasmas. Proc. Roy. Soc. (London), Ser. A, vol. 270, no. 1341, Nov. 13, 1962, pp. 155-167.
8. Norcross, D. W.; and Stone, P. M.: Recombination, Radiative Energy Loss and Level Populations in Nonequilibrium Cesium Discharges. J. Quant. Spectrosc. Radiat. Transfer, vol. 8, Feb. 1968, pp. 655-684.
9. Reichelt, W. H.; and Agnew, L.: Identification of the Ionic Species in a Cesium Plasma Diode. Thermionic Conversion Specialist Conference. IEEE, 1966, pp. 70-74.
10. Witting, H. L.: Mass Spectrometer Analysis of Cesium Ions from a Thermionic Converter. Thermionic Conversion Specialist Conference. IEEE, 1966, pp. 75-82.
11. Dugan, John V., Jr.: The Selection of Simple Model Atoms for Calculations of Electron Density in Non-Equilibrium, Low Temperature Cs Plasmas. Presented at the 27th Annual Conference for Physical Electronics, MIT, Cambridge, Mass., Mar. 20-22, 1967.
12. Warner, C.; and Hansen, L. K.: Transport Effects in the Electron-Rich Unignited Mode of Cesium Diodes. J. Appl. Phys., vol. 38, no. 2, Feb. 1967, pp. 491-500.
13. Stone, Philip M.: Cesium Oscillator Strengths. Phys. Rev., vol. 127, no. 4, Aug. 15, 1962, pp. 1151-1156. Erratum, Phys. Rev., vol. 135, no. 7AB, Sept. 28, 1964, p. 2.

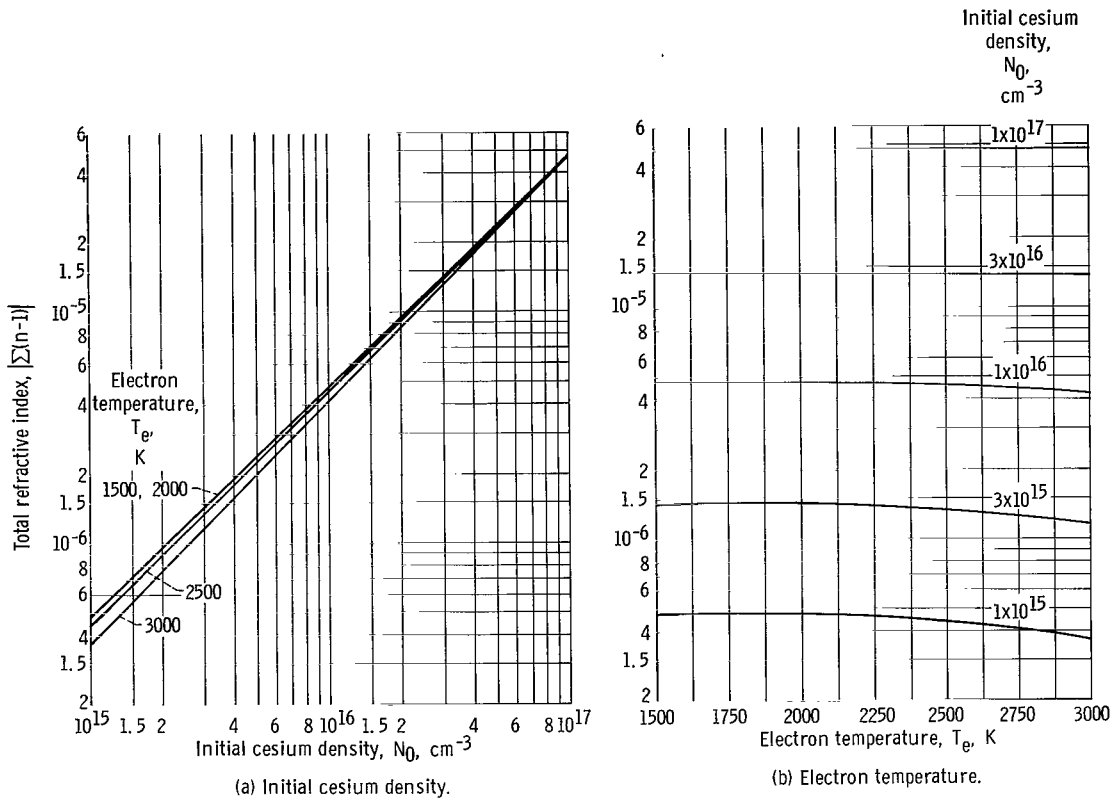


Figure 1. - Total refractive index at $0.6328 \mu\text{m}$ as function of initial cesium density.

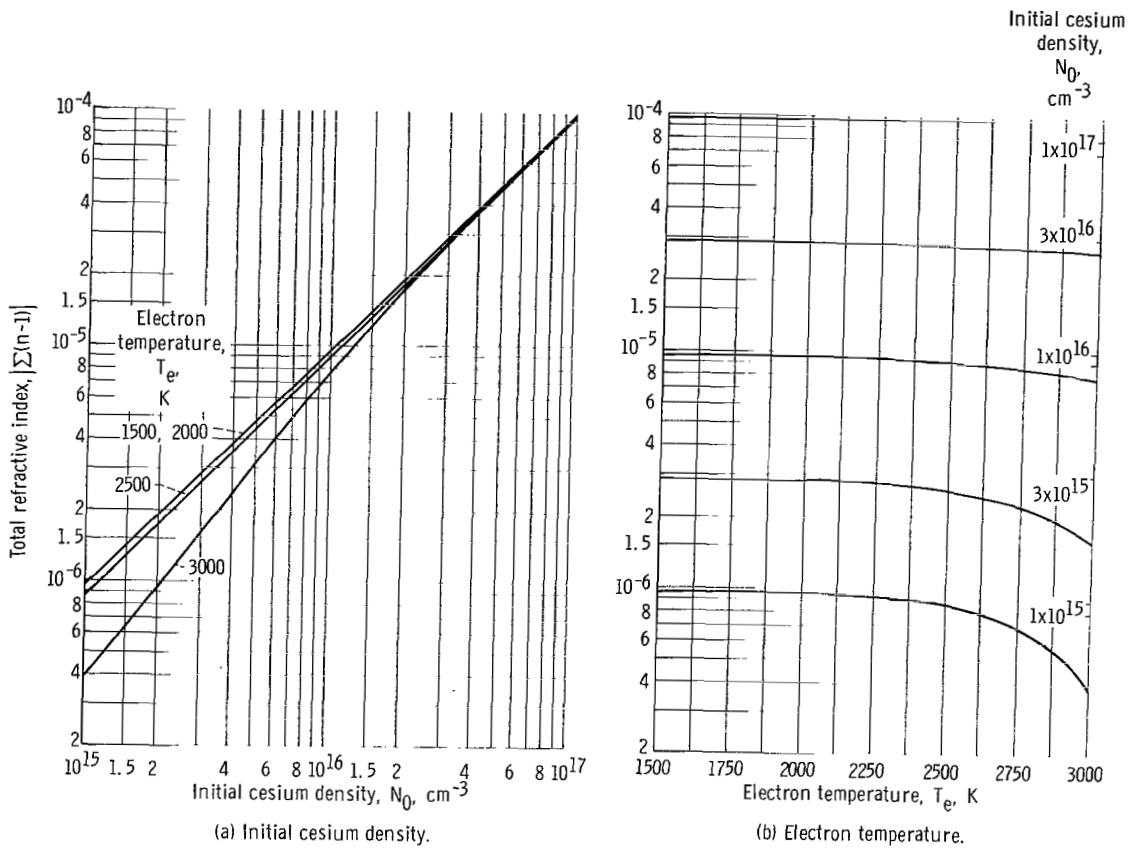


Figure 2 - Total refractive index at 1.523 μ m as function of initial cesium density.

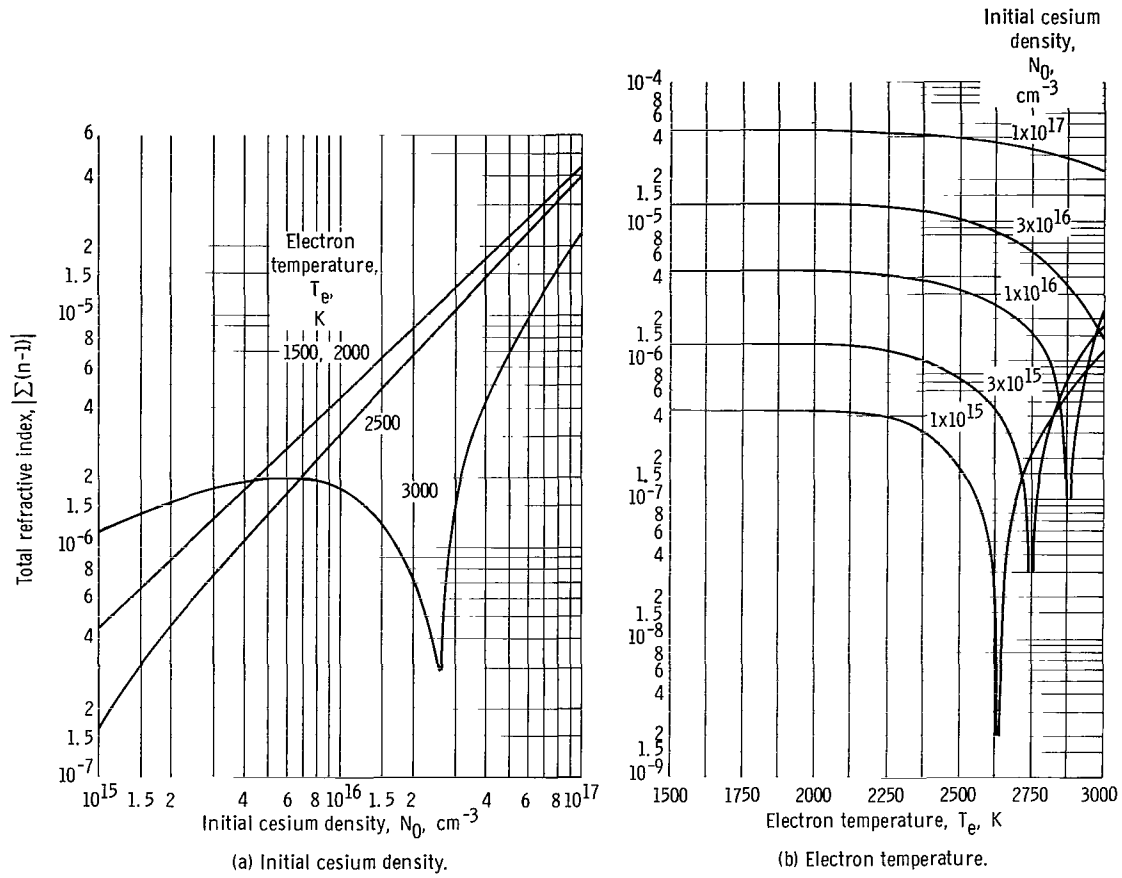


Figure 3. - Total refractive index at $3.3914 \mu\text{m}$ as function of initial cesium density.

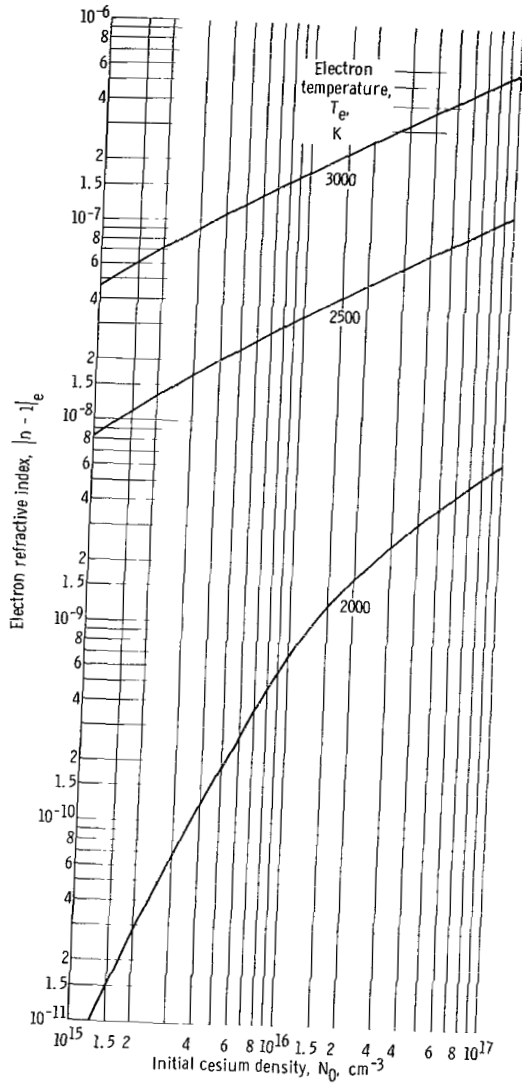


Figure 4. - Electron refractive index at $0.6328 \mu\text{m}$ as function of initial cesium density.

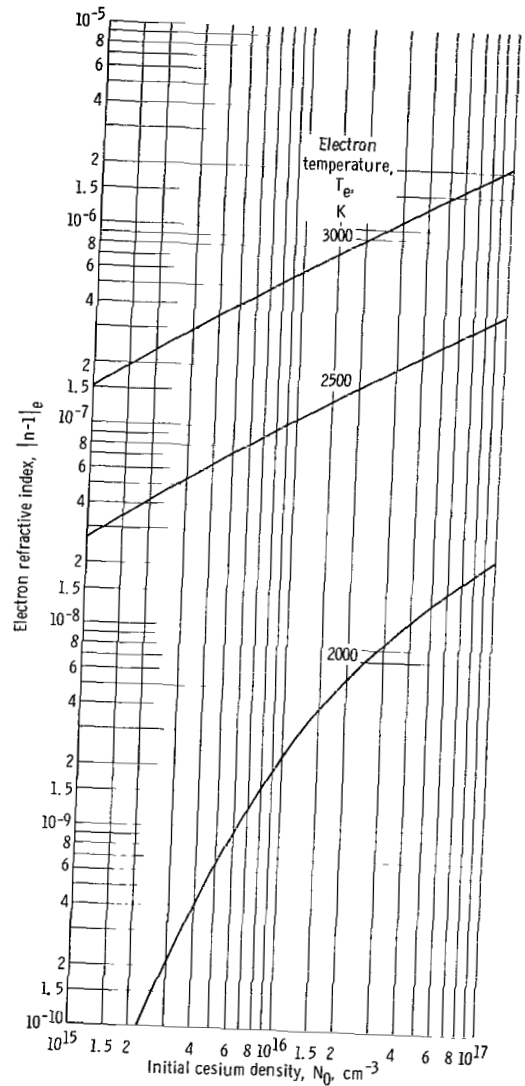


Figure 5. - Electron refractive index at $1.1523 \mu\text{m}$ as function of initial cesium density.

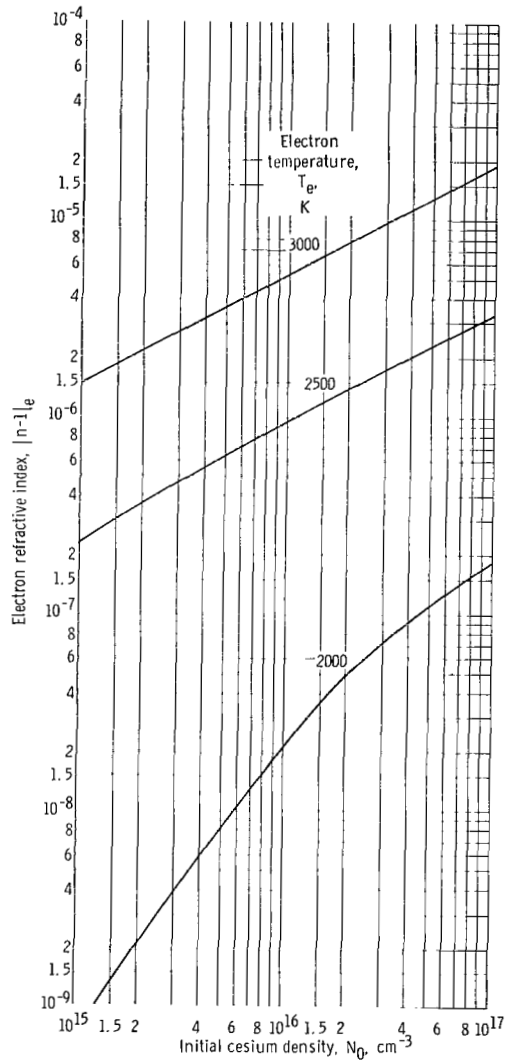


Figure 6. - Electron refractive index at $3.3914 \mu\text{m}$ as function of initial cesium density.

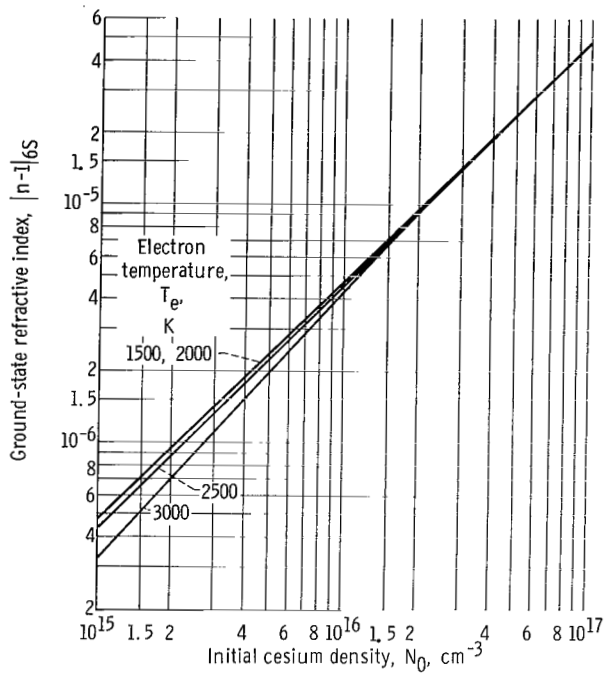


Figure 7. - Ground-state refractive index at 0.6328 μm as function of initial cesium density.

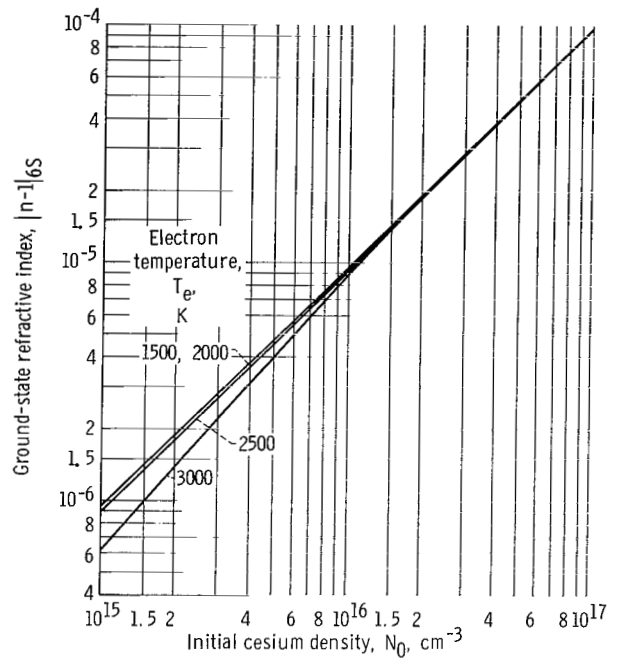


Figure 8. - Ground-state refractive index at 1.1523 μm as function of initial cesium density.

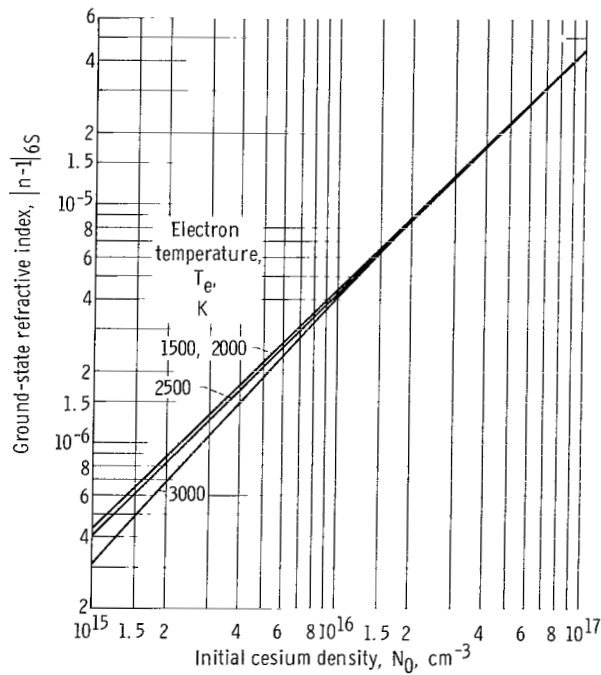


Figure 9. - Ground-state refractive index at 3.3914 μm as function of initial cesium density.

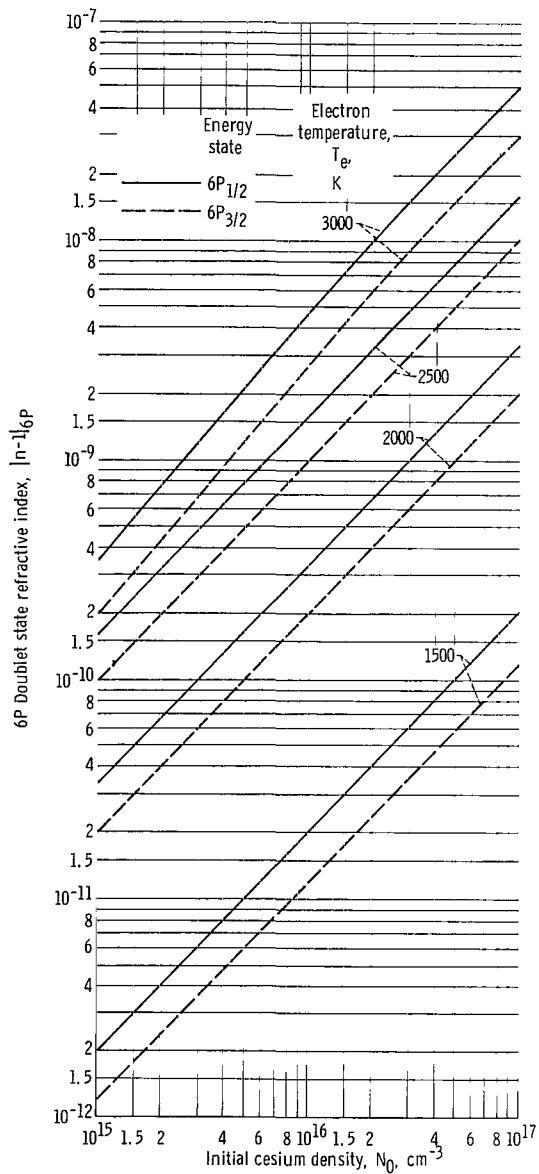


Figure 10. - 6P Doublet state refractive index at 0.6328 μm as function of initial cesium density.

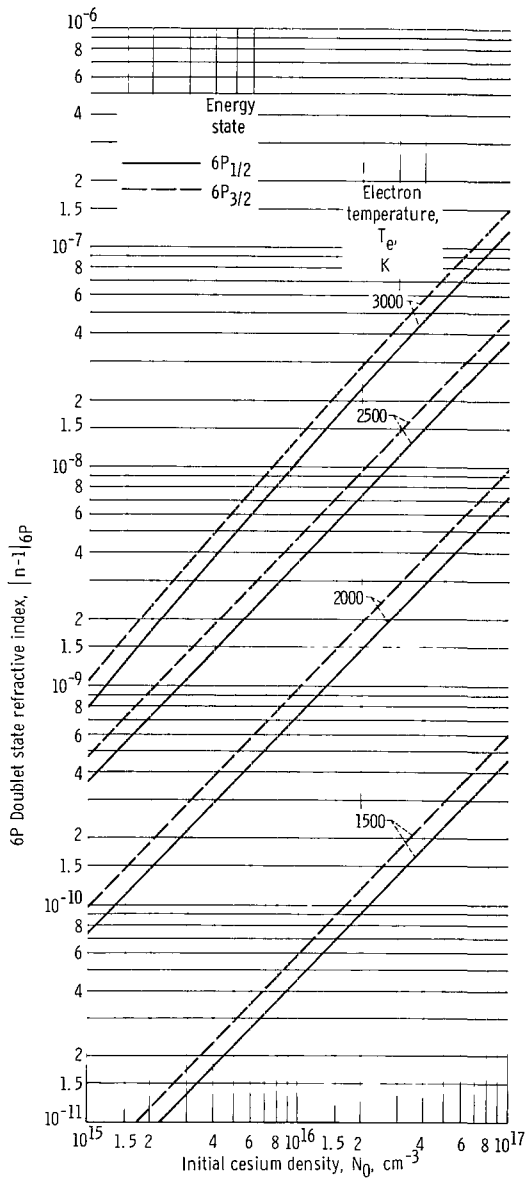


Figure 11. - 6P Doublet state refractive index at 1.1523 μm as function of initial cesium density.

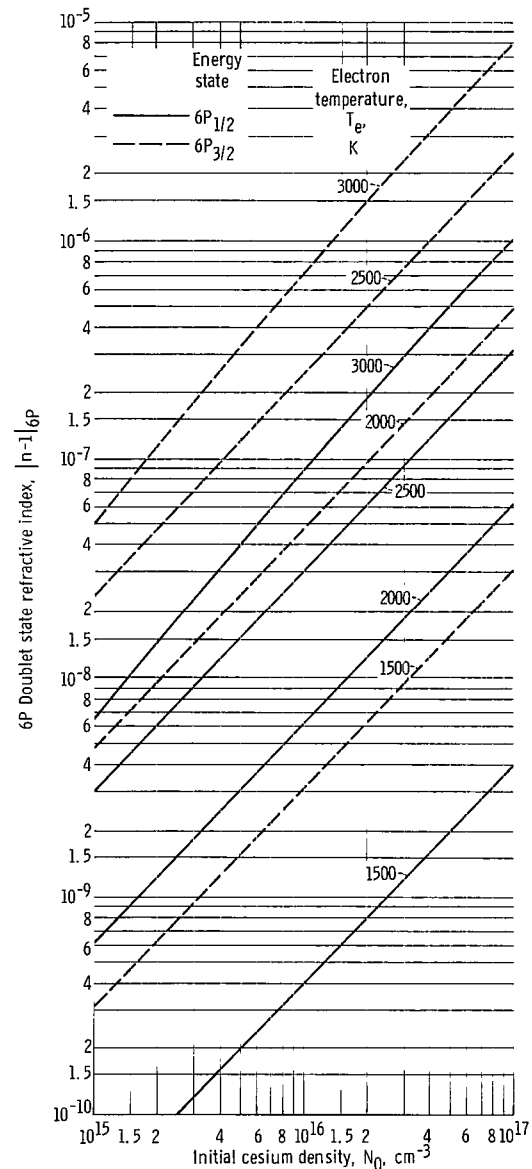


Figure 12. - 6P Doublet state refractive index at 3.3914 μm as function of initial cesium density.

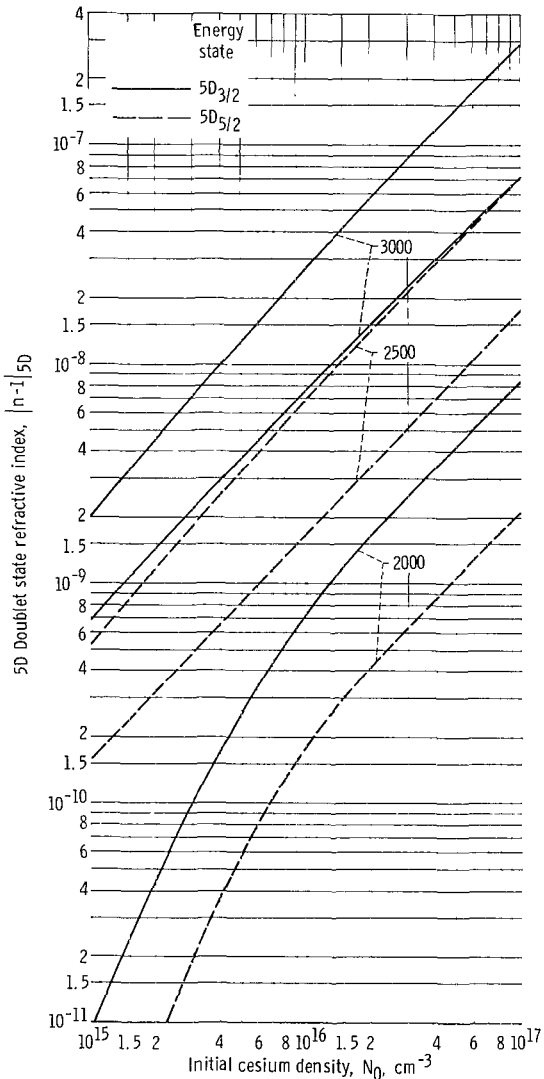


Figure 13. - 5D Doublet state refractive index at 0.6328 μm as function of initial cesium density.

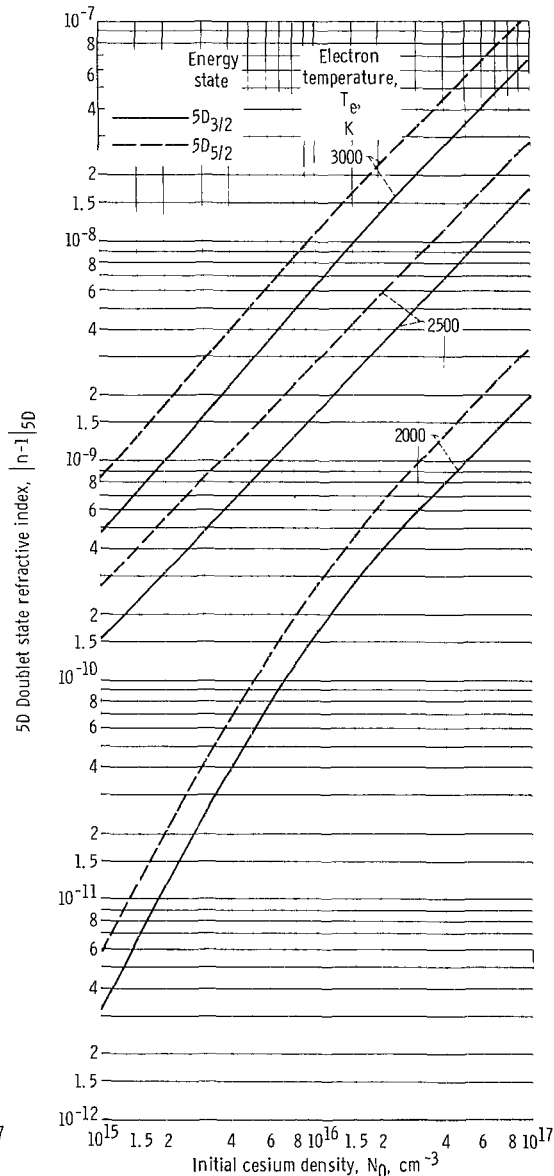


Figure 14. - 5D Doublet state refractive index at 1.1523 μm as function of initial cesium density.

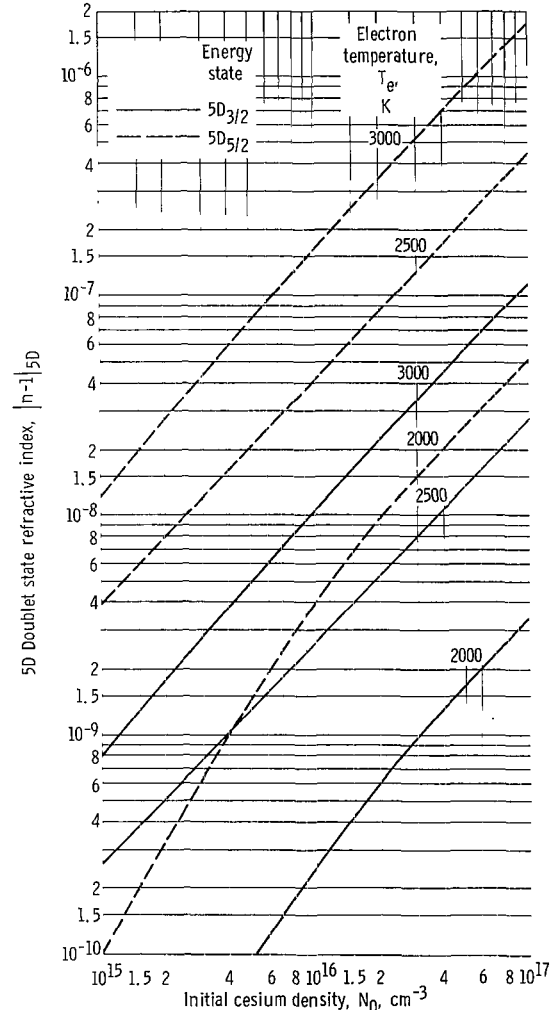


Figure 15. - 5D Doublet state refractive index at 3.3914 μm as function of initial cesium density.

FIRST CLASS MAIL



POSTAGE AND FEES PAID
NATIONAL AERONAUTICS AND
SPACE ADMINISTRATION

040 001 41 51 315 09176 00001
AIR FORCE WEAPON LABORATORY/AFWL/
KIRTLAND AIR FORCE BASE, NEW MEXICO 87117

SEE LISTING OF PUBLICATIONS ON THE BACK OF THIS MAILING

POSTMASTER: If Undeliverable (Section 158
Postal Manual) Do Not Return

"The aeronautical and space activities of the United States shall be conducted so as to contribute . . . to the expansion of human knowledge of phenomena in the atmosphere and space. The Administration shall provide for the widest practicable and appropriate dissemination of information concerning its activities and the results thereof."

— NATIONAL AERONAUTICS AND SPACE ACT OF 1958

NASA SCIENTIFIC AND TECHNICAL PUBLICATIONS

TECHNICAL REPORTS: Scientific and technical information considered important, complete, and a lasting contribution to existing knowledge.

TECHNICAL NOTES: Information less broad in scope but nevertheless of importance as a contribution to existing knowledge.

TECHNICAL MEMORANDUMS: Information receiving limited distribution because of preliminary data, security classification, or other reasons.

CONTRACTOR REPORTS: Scientific and technical information generated under a NASA contract or grant and considered an important contribution to existing knowledge.

TECHNICAL TRANSLATIONS: Information published in a foreign language considered to merit NASA distribution in English.

SPECIAL PUBLICATIONS: Information derived from or of value to NASA activities. Publications include conference proceedings, monographs, data compilations, handbooks, sourcebooks, and special bibliographies.

TECHNOLOGY UTILIZATION PUBLICATIONS: Information on technology used by NASA that may be of particular interest in commercial and other non-aerospace applications. Publications include Tech Briefs, Technology Utilization Reports and Notes, and Technology Surveys.

Details on the availability of these publications may be obtained from:

**SCIENTIFIC AND TECHNICAL INFORMATION DIVISION
NATIONAL AERONAUTICS AND SPACE ADMINISTRATION
Washington, D.C. 20546**